Bull. Mater. Sci. (2018) 41:38
https://doi.org/10.1007/s12034-018-1566-6

Facile synthesis and characterization of $CsPbBr_3$ and $CsPb_2Br_5$ powders

XINGHUA SU*, JING ZHANG and GE BAI
School of Materials Science and Engineering, Chang'an University, Xi'an 710061, China
*Author for correspondence (suxinghua@chd.edu.cn)

MS received 15 June 2017; accepted 10 August 2017; published online 23 March 2018

Abstract. All-inorganic caesium lead-halide perovskite $CsPbBr_3$ and $CsPb_2Br_5$ powders have emerged as attractive optoelectronic materials owing to their stabilities and highly efficient photoluminescence (PL). Herein we report a facile chemical route to prepare highly luminescent monoclinic $CsPbBr_3$ and tetragonal $CsPb_2Br_5$ powders at room temperature. The $CsPbBr_3$ powders exhibit regular crystal shape and demonstrate polyhedral geometry with an average particle size of 10 μm. The $CsPb_2Br_5$ powders show platelet morphologies and the lateral sizes of the particles are from 5 up to 200 μm. Both $CsPbBr_3$ and $CsPb_2Br_5$ powders present a narrow emission line-width and PL emission of 528 and 527 nm, respectively. A direct band gap of 2.35 eV and an indirect band gap of 3.01 eV are calculated for $CsPbBr_3$ and $CsPb_2Br_5$ powders, respectively. In addition, the monoclinic $CsPbBr_3$ can be transformed to tetragonal $CsPb_2Br_5$ in the presence of water. The large-scale synthesis of $CsPbBr_3$ and $CsPb_2Br_5$ will be advantageous in future applications of optoelectronic devices.

Keywords. $CsPbBr_3$; $CsPb_2Br_5$; powders; synthesis; characterization.

1. Introduction

Due to excellent charge transport properties [1] and broad chemical tenability [2], hybrid organic–inorganic lead halide-based perovskites have been broadly studied for potential applications in photovoltaic cells [3,4], light-emitting diodes (LEDs), lasers and photodetectors [5–10]. However, hybrid organic–inorganic perovskites are very sensitive to the environment, especially to water or moisture, which hinders large-scale practical and commercial applications [11,12]. Recently, the all-inorganic perovskites have been proposed as an alternative candidate for optoelectronics because of their higher chemical stability and unique electronic properties as compared with their hybrid organic–inorganic counterparts [13–15]. The general composition of all-inorganic perovskite is $CsPbX_3$ (X = Cl, Br and I), which has triggered a surge of investigations.

$CsPbBr_3$ and $CsPb_2Br_5$ are a kind of all-inorganic perovskites. Both of them have emerged as attractive semiconducting materials owing to their unique optoelectronic properties. Kulbak *et al* [16] prepared solar cells using $CsPbBr_3$ as a light absorber material. The solar cells showed performances comparable to those from the organic material, especially in generating high open circuit voltages. Pan *et al* [17] reported that $CsPbBr_3$ quantum dots (QDs) can produce high photoluminescence (PL) quantum yield with unprecedented operational stability in ambient conditions and high pump fluences. Song *et al* [18] for the first time reported QD LEDs based on all-inorganic perovskite $CsPbBr_3$, showing a promising luminescence intensity of 946 cd m^{-2}. Zhang *et al* [19] prepared LEDs using all-inorganic $CsPbBr_3$–$CsPb_2Br_5$ composite as the emitting layer, displaying a maximum luminance of 3853 cd m^{-2}, with current density of 8.98 cd A^{-1} and external quantum efficiency of 2.21%. Tang *et al* [20] reported that $CsPb_2Br_5$ microplates exhibited large optical gain and lasing emission under both one- and two-photon excitation, as well as enhanced stability.

Arising from the high performance, the synthesis and properties of $CsPbBr_3$ and $CsPb_2Br_5$ attract much attention. Traditionally, caesium lead-halide perovskites nanopowders have been prepared by the reaction of $PbBr_2$ with metal–organic complex in organic solvent (for example, octadecene and oleylamine) at relatively high temperature [20–22]. However, the metal–organic complex decomposition is a complex, expensive and limited-scale synthesis method. The growing interest in caesium lead-halide perovskites motivates us to develop simple and cheap alternative methods for large-scale synthesis of $CsPbBr_3$ and $CsPb_2Br_5$ powders.

In this article, we report a facile precipitation route for synthesis of $CsPbBr_3$ and $CsPb_2Br_5$ powders in aqueous solution. The process is quite simple, so that the production rate is expected to be much higher than those of other methods. Detailed crystal structural characterization reveals that $CsPbBr_3$ and $CsPb_2Br_5$ powders crystallize in a monoclinic and tetragonal phase, respectively. Optical measurements show that both $CsPbBr_3$ and $CsPb_2Br_5$ display strong PL. These powders have potential applications in optoelectronics.

2. Experimental

2.1 *Preparation of $CsPbBr_3$ and $CsPb_2Br_5$ powders*

Lead(II) acetate trihydrate ($Pb(CH_3COO)_2 \cdot 3H_2O$) (Macklin Chemical, China, purity: 99.5%), hydrobromic acid (HBr) (Macklin Chemical, China, 40% w/w) and caesium bromide (CsBr) (Macklin Chemical, China, purity: 99.5%) were selected as the starting materials.

First, lead(II) acetate trihydrate was fully dissolved in hydrobromic acid at room temperature to obtain solution I. Caesium bromide was fully dissolved in a blend solution of hydrobromic acid and deionized water at room temperature to obtain solution II. Later, solution II was added slowly into solution I with successive stirring. The mole ratio of Cs^+/Pb^{2+} in mixed solution was adjusted to 1/1, 2/1 and 1/2. The obtained products were washed by diethyl ether three times, and were dried in vacuum for 12 h.

2.2 *Characterization*

The X-ray diffraction (XRD) measurements of the powders were performed with an X-ray diffractometer (Bruker D8 Davinci, Germany) with Cu K_α radiation (40 kV, 60 mA) in the range of 2θ = 10–50°. The scan was performed at a scan rate of 5° min^{-1} with the step size of 0.02°. The morphologies of the powders were examined by field emission scanning electron microscopy (SEM, Hitachi S-4800, Tokyo, Japan). The PL spectra were measured using a 473 nm solid-state laser for excitation, detected using a grating spectrometer. UV–Vis absorption spectra were collected using a Hitachi-U2001 spectrophotometer in the reflectance mode.

3. Results and discussion

The phases of powders obtained with various mole ratios of Cs^+/Pb^{2+} in the solution are studied. Figure 1 shows the XRD pattern of sample obtained with Cs^+/Pb^{2+} mole ratio of 1/1. It is found that the diffraction peaks of monoclinic $CsPbBr_3$ (PDF#18-0364) and tetragonal $CsPb_2Br_5$ (PDF#25-0211) coexist in the sample. As the Cs^+/Pb^{2+} mole ratio of rises to 2/1, the diffraction peaks of tetragonal $CsPb_2Br_5$ disappear completely, and only diffraction peaks of monoclinic $CsPbBr_3$ can be observed, as shown in figure 2. The as-obtained monoclinic $CsPbBr_3$ powders show an orange colour. When the Cs^+/Pb^{2+} mole ratio decreases to 1/2, the XRD pattern (figure 3) contains the sharp diffraction peaks of tetragonal $CsPb_2Br_5$, indicating that well-crystallized tetragonal $CsPb_2Br_5$ powder is prepared. The as-obtained tetragonal $CsPb_2Br_5$ powder shows a white colour.

Based on the results of the XRD analysis, it can be seen that the Cs^+/Pb^{2+} mole ratio has an effect on the phase of final product in this synthesis process. Generally speaking, the reaction that occurs for the formation of $CsPbBr_3$ by CsBr and $PbBr_2$ is

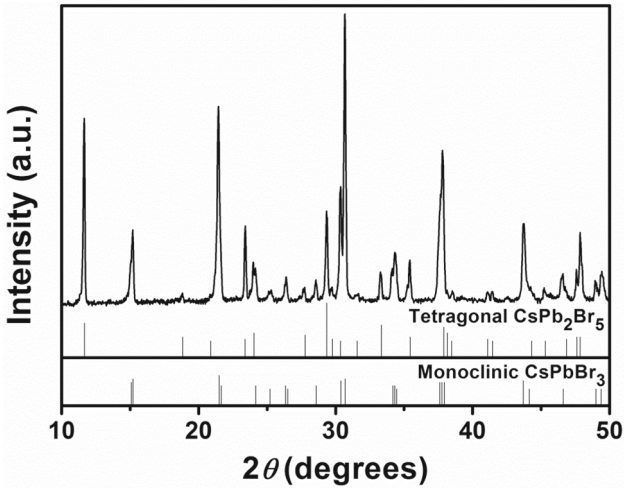

Figure 1. XRD pattern of powders obtained at a Cs^+/Pb^{2+} mole ratio of 1/1.

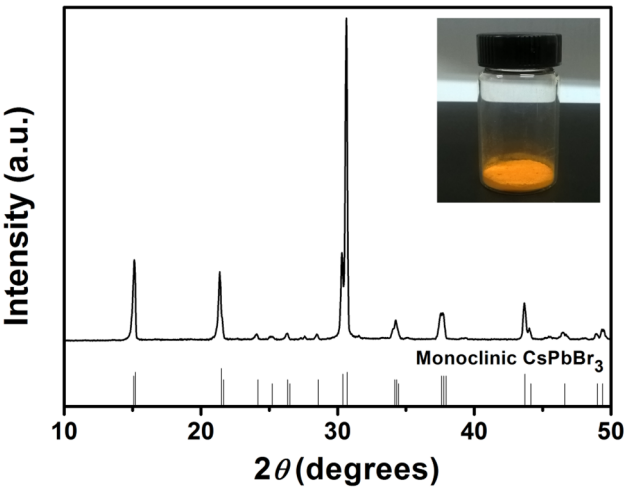

Figure 2. XRD pattern of powders obtained at a Cs^+/Pb^{2+} mole ratio of 2/1. Inset is photographs of as-obtained $CsPbBr_3$ powders.

$$CsBr + PbBr_2 \rightarrow CsPbBr_3 \quad (1)$$

According to this reaction, as the Cs^+/Pb^{2+} mole ratio is 1/1, the product should be pure $CsPbBr_3$. However, the real product is a mixture of monoclinic $CsPbBr_3$ and tetragonal $CsPb_2Br_5$ (figure 1). Pure $CsPbBr_3$ powder can be prepared when the Cs^+/Pb^{2+} mole ratio is 2/1 (figure 2). Intriguingly, when the Cs/Pb mole ratio is 1/2, pure $CsPb_2Br_5$ can be obtained, in accordance with the reaction

$$CsBr + 2PbBr_2 \rightarrow CsPb_2Br_5 \quad (2)$$

Here, it is believed that at the conditions of this synthesis, different Cs^+/Pb^{2+} mole ratios lead to modification of the solution environment, resulting in a change in the

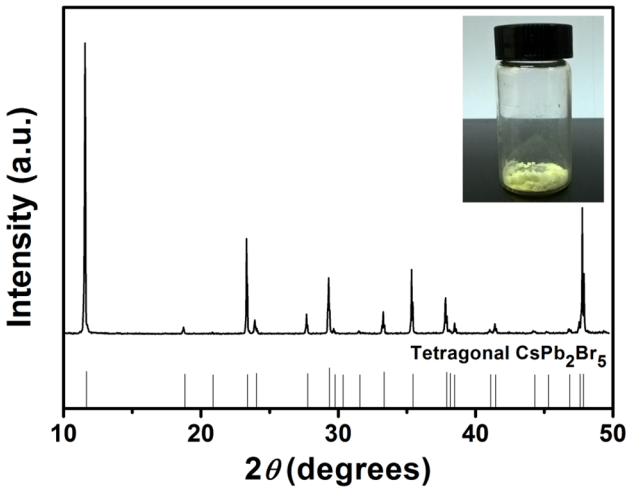

Figure 3. XRD pattern of powders obtained at a Cs^+/Pb^{2+} mole ratio of 1/2. Inset is photographs of as-obtained $CsPb_2Br_5$ powders.

thermodynamically favoured phase of the caesium lead halide. Therefore, in this work, the Cs^+/Pb^{2+} mole ratio influences the phase of final product.

It is reported that caesium lead bromide belongs to the family of trihalides compounds, in which several successive phase transitions occur between room temperature and melting temperatures. $CsPbBr_3$ crystallizes in monoclinic polymorph at room temperature and with rising temperature it transforms to tetragonal phase. Above 130°C, $CsPbBr_3$ crystallizes in cubic polymorph with the perovskite structure [23,24]. The existing methods for $CsPbBr_3$ nanopowders are normally at the high synthesis temperature of 150 or 170°C, producing a cubic perovskite phase [25,26]. In this work, the $CsPbBr_3$ crystallizes in the monoclinic phase, which can be attributed to the room temperature synthesis.

The morphologies of the $CsPbBr_3$ and $CsPb_2Br_5$ powders synthesized are shown in figure 4. Both of the $CsPbBr_3$ and $CsPb_2Br_5$ powders are well separated. The $CsPbBr_3$ powders have regular crystal shape and demonstrate polyhedral geometry. The average particle size of $CsPbBr_3$ powders are 10 μm (figure 4a). The $CsPb_2Br_5$ powders show platelet morphologies and the lateral sizes of the particles are from 5 up to 200 μm (figure 4b).

It is well known that the crystal growth behaviour is determined by the intrinsic symmetry of its crystal structure. Therefore, the different morphologies of $CsPbBr_3$ and $CsPb_2Br_5$ powders in this synthesis process result from their different intrinsic symmetries of the crystal structures. The monoclinic phase of $CsPbBr_3$ presents a perovskite structure, in which the $\{PbBr_6\}^{4-}$ octahedron extends to three dimensions via sharing the vertex and Cs^+ ions localize in the octahedral voids, as shown in figure 5a. Figure 5b shows the crystal structure of the tetragonal $CsPb_2Br_5$. It is found that one layer of Cs^+ ion is sandwiched between two layers of $[Pb_2Br_5]^-$. The features of the tetragonal $CsPb_2Br_5$

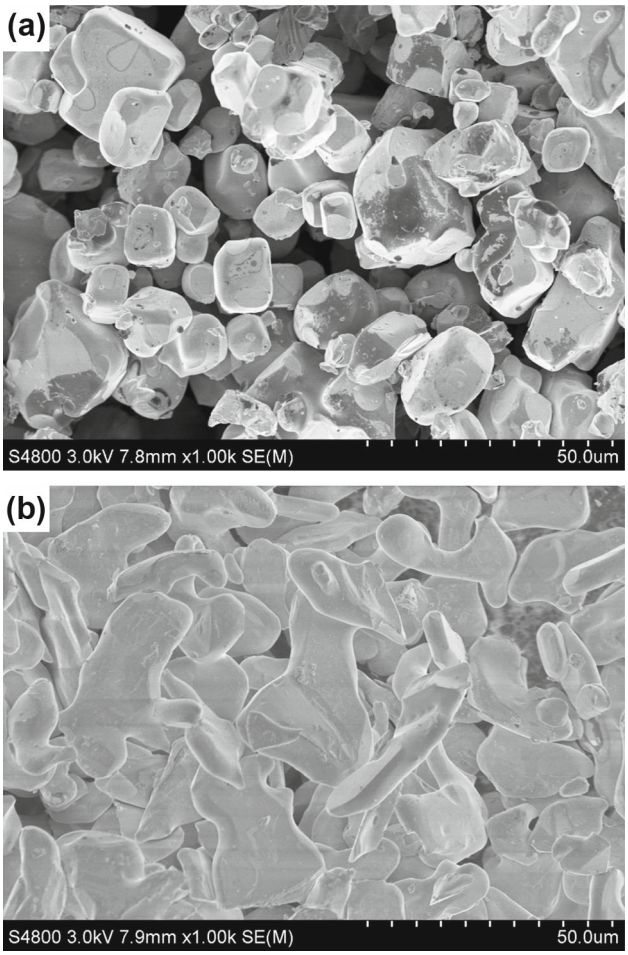

Figure 4. SEM micrographs of **(a)** $CsPbBr_3$ and **(b)** $CsPb_2Br_5$ powders.

crystal structure are similar to that of layered double hydroxides, whose platelet morphology has been easily obtained by the facile precipitation method [27].

In order to study the chemical stability of $CsPbBr_3$ in water, distilled water is added to the $CsPbBr_3$ powders. Figure 6 shows the colour changes of $CsPbBr_3$ powders soaked in water. It can be seen that the initial orange colour changes to white colour completely in 90 s, illustrating that $CsPbBr_3$ is very sensitive to water and $CsPbBr_3$ transforms to a new phase in the presence of water. To further investigate the phase transformation of $CsPbBr_3$ in water, the crystal structures of obtained white product and material obtained by drying the clear supernatant (figure 6) are analysed. As shown in figures 7 and 8, the white product is characterized as tetragonal $CsPb_2Br_5$ (PDF#25-0211), and the matter obtained by drying the clear supernatant is confirmed as cubic CsBr (PDF# 73-0391). According to the results of XRD analysis (figures 7 and 8), it is proposed that $CsPbBr_3$ decomposes to $CsPb_2Br_5$ and CsBr in the presence of water, which occurs as follows:

$$2CsPbBr_3 \rightarrow CsPb_2Br_5 + CsBr \quad (3)$$

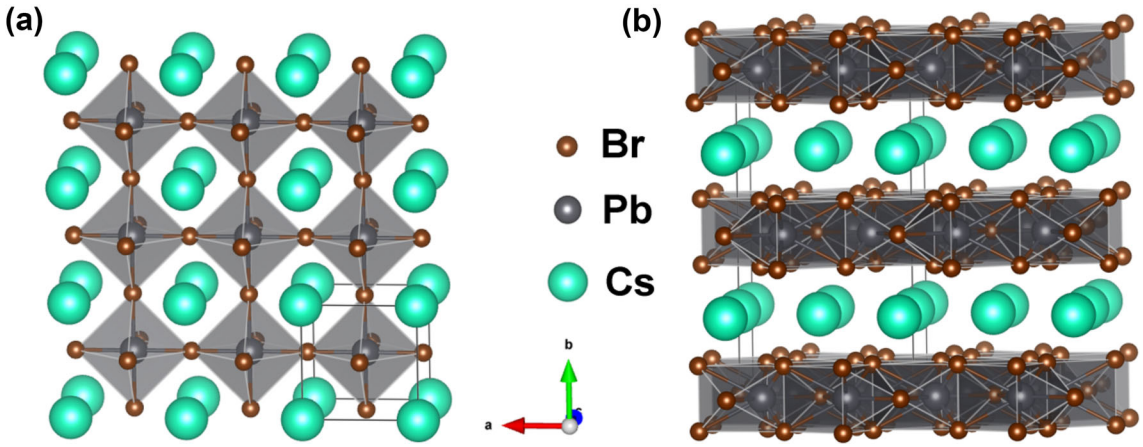

Figure 5. Perovskite crystal structure of **(a)** $CsPbBr_3$ and **(b)** perovskite-related crystal structure of $CsPb_2Br_5$.

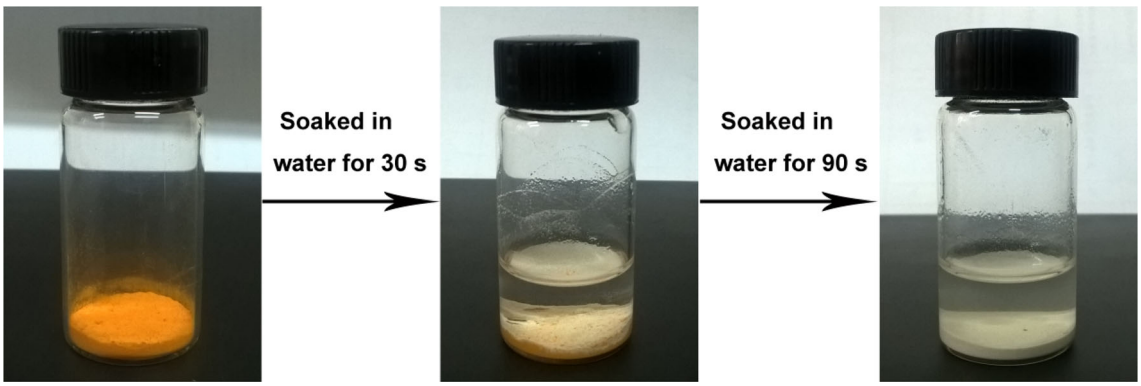

Figure 6. Photograph of the colour changes of $CsPbBr_3$ powders soaked in water.

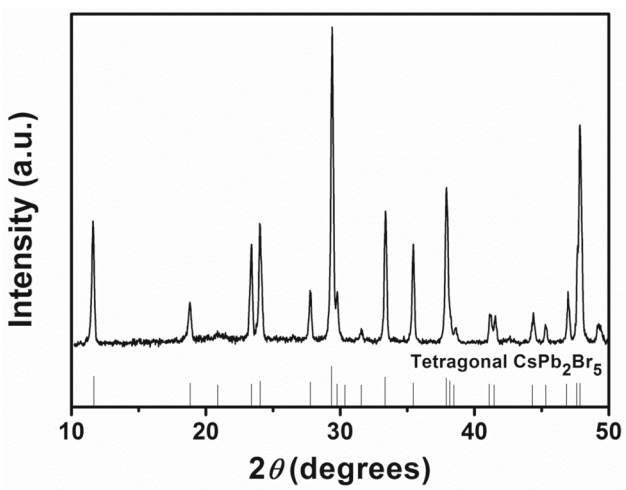

Figure 7. XRD pattern of the white product shown in figure 6.

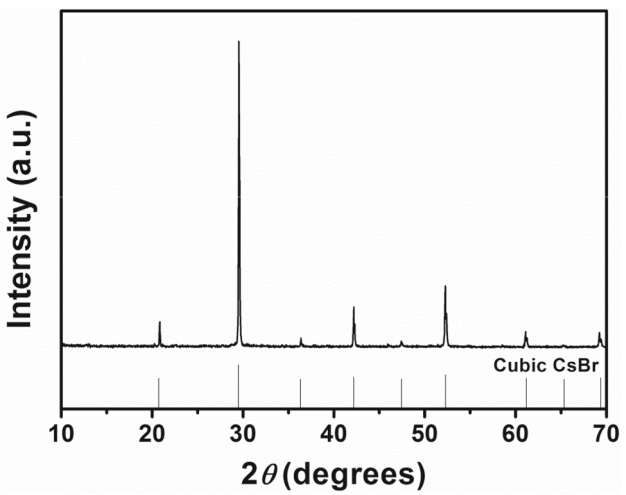

Figure 8. XRD pattern of material obtained by drying the clear supernatant shown in figure 6.

In this reaction process, water can be acted as a catalyser, as reported in the decomposition of organic–inorganic hybrid perovskite $CH_3NH_3PbI_3$ [11,28].

The optical properties of the $CsPbBr_3$ and $CsPb_2Br_5$ powders are studied by measuring the UV–Vis absorption and PL spectra. Figure 9a shows the UV–Vis adsorption and PL

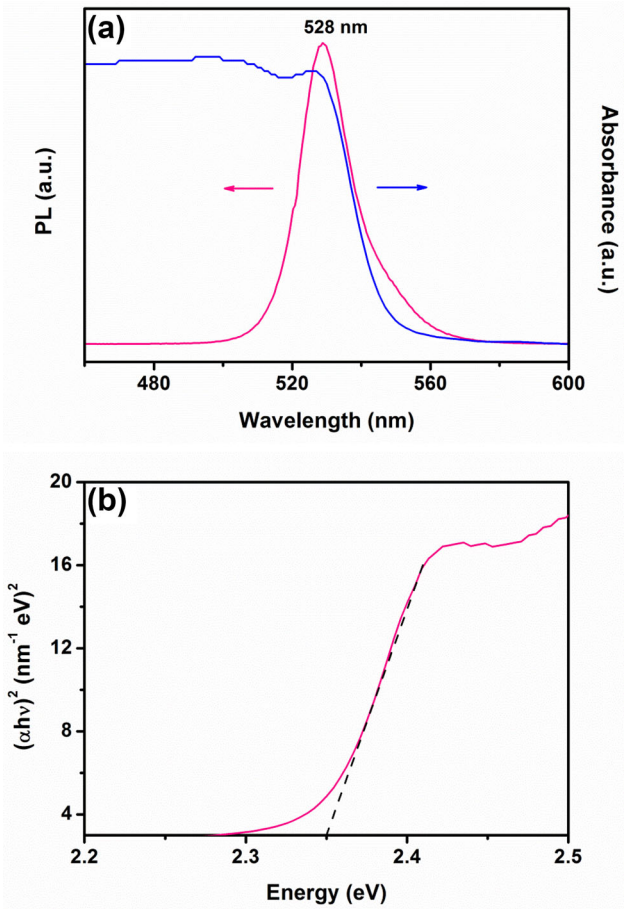

Figure 9. Absorption (right) and PL (left) spectra of **(a)** $CsPbBr_3$ powders, and **(b)** direct band gap Tauc plot of $CsPbBr_3$ from absorption spectrum. The PL under 473 nm excitation.

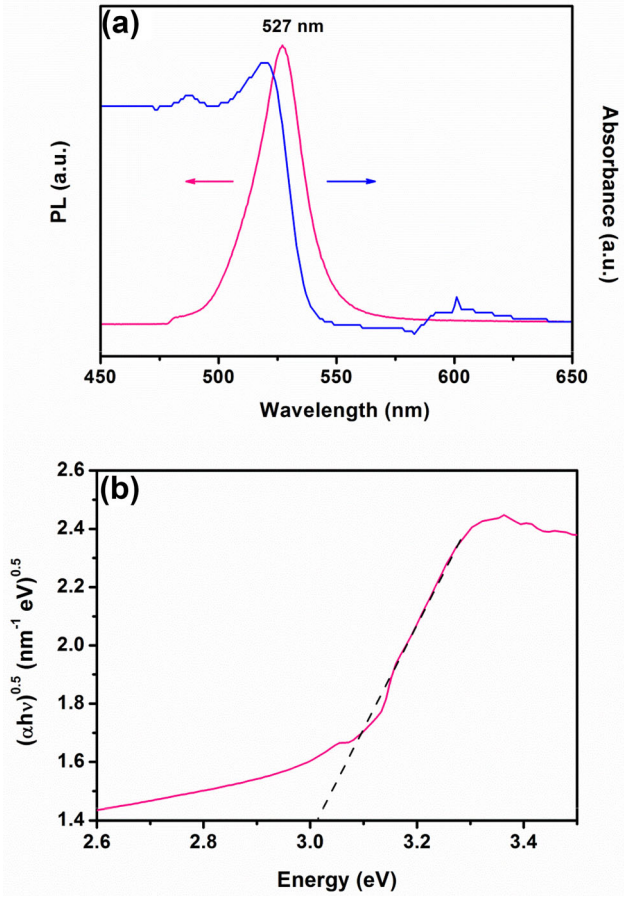

Figure 10. Absorption (right) and PL (left) spectra of **(a)** $CsPb_2Br_5$ powders, and **(b)** indirect band gap Tauc plot of $CsPb_2Br_5$ from absorption spectrum. The PL under 473 nm excitation.

emission spectra of $CsPbBr_3$ powders. The absorption onset for the $CsPbBr_3$ is found to be 521 nm. The PL emission spectrum of $CsPbBr_3$ exhibits a peak at 528 nm with a narrow full-width at half-maximum (FWHM) of 16 nm, which is similar to the optical features of $CsPbBr_3$ nanocrystals [29]. The direct band gap Tauc plot of $CsPbBr_3$ from absorption spectrum gives a direct gap of 2.35 eV, as shown in figure 9b. The optical absorption and PL emission spectra of $CsPb_2Br_5$ powders are shown in figure 10a, from which we can see a small Stokes shift, and the highly symmetric PL peak centres at 527 nm with a narrow FWHM of 12 nm, indicating its potential application for lasing. According to the absorption spectrum, an indirect band gap of 3.01 eV is calculated (figure 10b), which is in accordance with the reported results [30].

The PL property of microsized $CsPbBr_3$ powders obtained in this work is different from that of QDs. Pan *et al* [17] prepared $CsPbBr_3$ QDs with average sizes of 8.2, 9.2 and 10.6 nm; the PL positions of these samples are 496, 503 and 512 nm, respectively, implying that PL peak shifts to longer wavelength when the size of QDs is increased. These results are due to the quantum confinement. The typical PL peak of the $CsPbBr_3$ QDs in their work is 512 nm. Besides, Song *et al* [18] reported that the typical PL peak of the $CsPbBr_3$ QDs was located at 510 nm. In this work, the microsized $CsPbBr_3$ powders present a PL emission of 528 nm. These results demonstrate that the PL emission wavelength of microsized $CsPbBr_3$ powders is longer than that of $CsPbBr_3$ QDs. However, there is no obvious difference between PL properties of microsized and nanosized $CsPb_2Br_5$ powders. Ruan *et al* [31] reported that PL emission spectrum of $CsPb_2Br_5$ nanowires showed a peak at 525 nm. Meanwhile, the PL emission peak position of $CsPb_2Br_5$ nanosheets was at 529 nm. The microsized $CsPb_2Br_5$ powders obtained in our work have a PL emission peak at 527 nm. It can be concluded that the PL property of microsized $CsPb_2Br_5$ powders is similar to that of nanosized $CsPb_2Br_5$ particles.

4. Conclusions

A facile and scalable method for the synthesis of highly luminescent $CsPbBr_3$ and $CsPb_2Br_5$ powders is reported. The Cs^+/Pb^{2+} mole ratio has a significant effect on the phase

of final product in the synthesis process. Both $CsPbBr_3$ and $CsPb_2Br_5$ powders present a narrow emission line-width and PL emission at 528 and 527 nm, respectively. These $CsPbBr_3$ and $CsPb_2Br_5$ powders have potential applications in optoelectronic devices.

Acknowledgements

This work was supported by the China Postdoctoral Science Foundation under Grant Number 2015M582584, the Postdoctoral Research Project of Shaanxi Province under Grant Number 2016BSHEDZZ06, the Special Fund for Basic Scientific Research of Central Colleges, Chang'an University, under Grant Number 310831171011 and the Special Fund for Basic Research Support Programs of Chang'an University.

References

[1] Dong Q, Fang Y, Shao Y, Mulligan P, Qiu J, Cao L and Huang J 2015 *Science* **347** 967
[2] Noh J H, Im S H, Heo J H, Mandal T N and Seok S I 2013 *Nano Lett.* **13** 1764
[3] Liu M, Johnston M B and Snaith H J 2013 *Nature* **501** 395
[4] Yang W S, Noh J H, Jeon N J, Kim Y C, Ryu S, Seo J *et al* 2015 *Science* **348** 1234
[5] Tan Z K, Moghaddam R S, Lai M L, Docampo P, Higler R, Deschler F *et al* 2014 *Nat. Nanotechnol*. **9** 687
[6] Kim Y H, Cho H, Heo J H, Kim T S, Myoung N, Lee C L *et al* 2015 *Adv. Mater*. **27** 1248
[7] Zhang Q, Ha S T, Liu X, Sum T C and Xiong Q 2014 *Nano Lett*. **14** 5995
[8] Sutherland B R, Hoogland S, Adachi M M, Wong C T and Sargent E H 2014 *ACS Nano* **8** 10947
[9] Hu X, Zhang X, Liang L, Bao J, Li S, Yang W *et al* 2014 *Adv. Funct. Mater*. **24** 7373
[10] Dou L, Yang Y M, You J, Hong Z, Chang W H, Li G *et al* 2014 *Nat. Commun*. **5** 5404
[11] Zhu Z, Hadjiev V G, Rong Y, Guo R, Cao B, Tang Z *et al* 2016 *Chem. Mater*. **28** 7385
[12] Gu Z, Wang K, Sun W, Li J, Liu S, Song Q *et al* 2016 *Adv. Opt. Mater*. **4** 472
[13] Song J, Xu L, Li J, Xue J, Dong Y, Li X *et al* 2016 *Adv. Opt. Mater*. **28** 4861
[14] Li X, Wu Y, Zhang S, Cai B, Gu Y, Song J *et al* 2016 *Adv. Funct. Mater*. **26** 2435
[15] Swarnkar A, Chulliyil R, Ravi V K, Irfanullah M, Chowdhury A and Nag A 2015 *J Angew. Chem. Int. Ed*. **54** 15424
[16] Kulbak M, Cahen D and Hodes G 2015 *J. Phys. Chem. Lett*. **6** 2452
[17] Pan J, Sarmah S P, Murali B, Dursun I, Peng W, Parida M R *et al* 2015 *J. Phys. Chem. Lett*. **6** 5027
[18] Song J, Li J, Li X, Xu L, Dong Y and Zeng H 2015 *Adv. Mater*. **27** 7162
[19] Zhang X, Xu B, Zhang J, Gao Y, Zheng Y, Wang K *et al* 2016 *Adv. Funct. Mater*. **26** 4595
[20] Tang X, Hu Z, Yuan W, Hu W, Shao H, Han D *et al* 2017 *Adv. Opt. Mater*. **5** 1600788
[21] Akkerman Q A, Motti S G, Kandada A R S, Mosconi E, D'Innocenzo V, Bertoni G *et al* 2016 *J. Am. Chem. Soc*. **138** 1010
[22] Bekenstein Y, Koscher B A, Eaton S W, Yang P and Alivisatos A P 2015 *J. Am. Chem. Soc*. **137** 16008
[23] Rodová M, Brožek J, Knížek K and Nitsch K 2003 *J. Therm. Anal. Calorim*. **71** 667
[24] Møller C K 1958 *Nature* **182** 1436
[25] Protesescu L, Yakunin S, Bodnarchuk M I, Krieg F, Caputo R, Hendon C H *et al* 2015 *Nano Lett*. **15** 3692
[26] Shamsi J, Dang Z, Bianchini P, Canale C, Stasio F D, Brescia R *et al* 2016 *J. Am. Chem. Soc*. **138** 7240
[27] Ma R, Liu Z, Takada K, Iyi N, Bando Y and Sasaki T 2007 *J. Am. Chem. Soc*. **129** 5257
[28] Niu G D, Guo X D and Wang L D 2015 *J. Mater. Chem. A* **3** 8970
[29] Tang X, Hu Z, Chen W, Xing X, Zang Z, Hu W *et al* 2016 *Nano Energy* **28** 462
[30] Li G, Wang H, Zhu Z, Chang Y, Zhang T, Song Z *et al* 2016 *Chem. Commun*. **52** 11296
[31] Ruan L, Shen W, Wang A, Xiang A and Deng Z 2017 *J. Phys. Chem. Lett*. **8** 3853